

Supplementary Materials

NiS nanoparticle-MoS₂ nanosheet core-shell spheres: PVP-assisted synthesis and efficient electrocatalyst for hydrogen evolution reaction

Gabriel Engonga Obiang Nsang¹, Badshah Ullah¹, Sun Hua¹, Sayyar Ali Shah^{1,4,*}, Nabi Ullah², Noor Ullah¹, Flora Ngozi Dike¹, Waleed Yaseen³, Aihua Yuan^{1,*}, Naseem Khan¹, Habib Ullah^{4,*}

¹School of Environmental & Chemical Engineering, Jiangsu University of Science and Technology, Zhenjiang 212003, Jiangsu, China.

²Department of Inorganic and Analytical Chemistry, Faculty of Chemistry, University of Lodz, Tamka 12, Lodz 91-403, Poland.

³School of Chemistry and Chemical Engineering, Jiangsu University, Zhenjiang 212013, Jiangsu, China.

⁴Department of Engineering, Faculty of Environment, Science and Economy, University of Exeter, Exeter EX4 4QF, UK.

Correspondence to: Dr. Sayyar Ali Shah, School of Environmental & Chemical Engineering, Jiangsu University of Science and Technology, Zhenjiang 212003, Jiangsu, China; Department of Engineering, Faculty of Environment, Science and Economy, University of Exeter, Exeter EX4 4QF, UK. E-mail: sayyarali83@just.edu.cn; Dr. Aihua Yuan, School of Environmental & Chemical Engineering, Jiangsu University of Science and Technology, Zhenjiang 212003, Jiangsu, China. E-mail: aihua.yuan@just.edu.cn; Dr. Habib Ullah, Department of Engineering, Faculty of Environment, Science and Economy, University of Exeter, Exeter EX4 4QF, UK. E-mail: Hu203@exeter.ac.uk

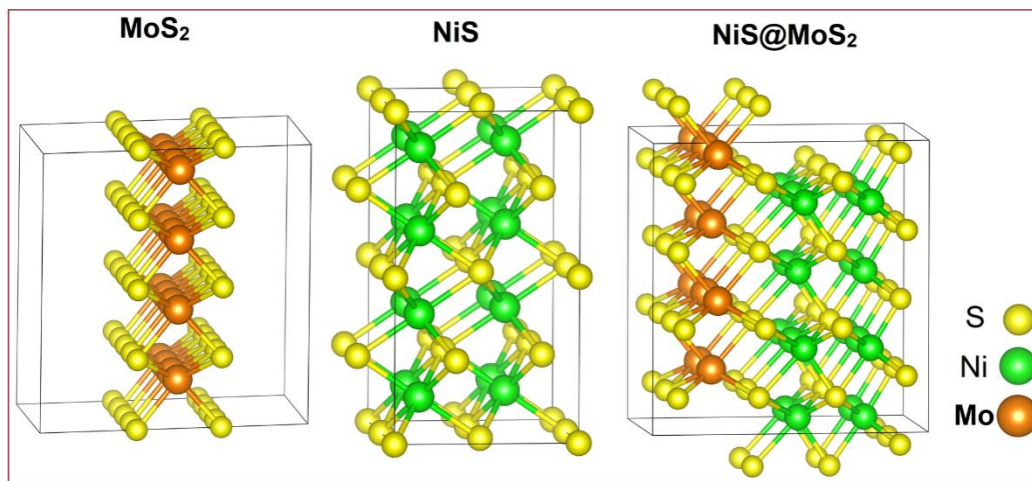


Fig. S1. Optimized structures for MoS₂, NiS, and the heterojunction NiS@MoS₂.

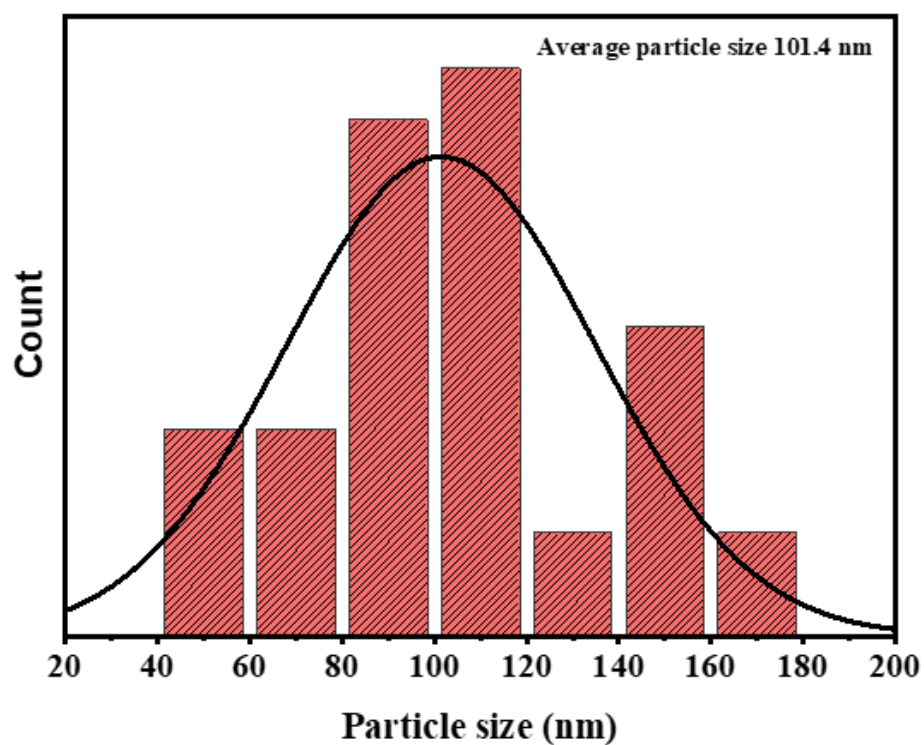


Fig. S2. Histogram showing the sphere size distribution of the SEM image of the NiS@MoS₂/NC₅₀ composite.

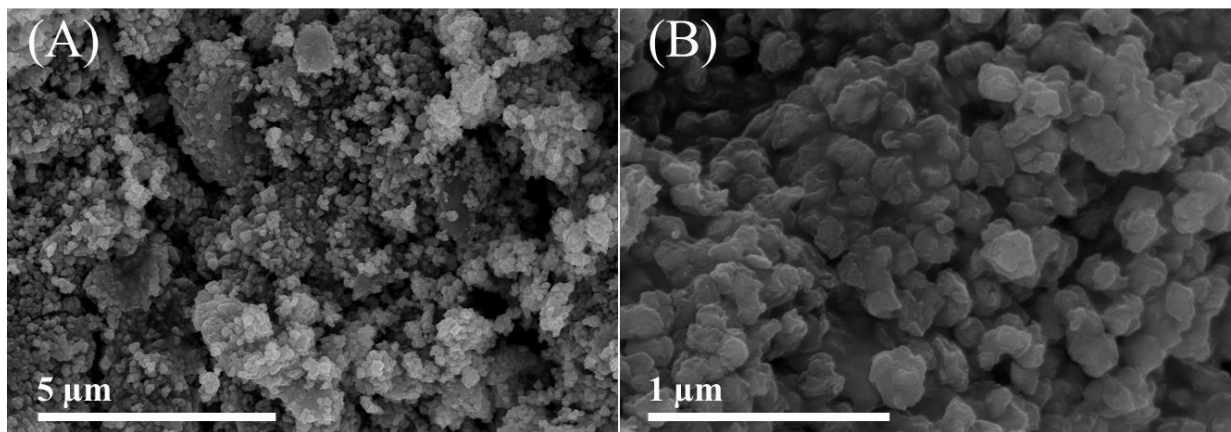


Fig. S3. SEM of the NiS@MoS₂/NC₂₅ composite at lower and higher magnification respectively.

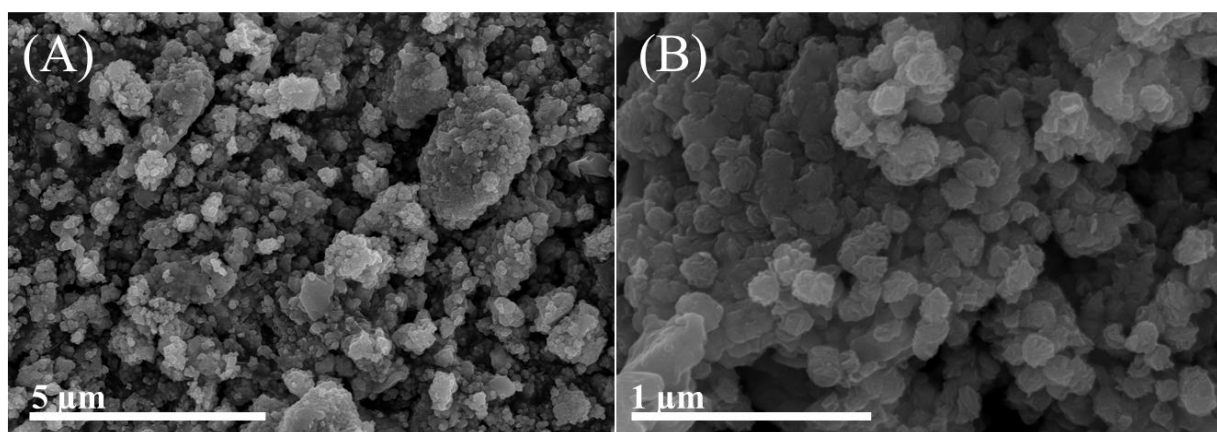


Fig. S4. SEM of the NiS@MoS₂/NC₇₅ composite at lower and higher magnification respectively.

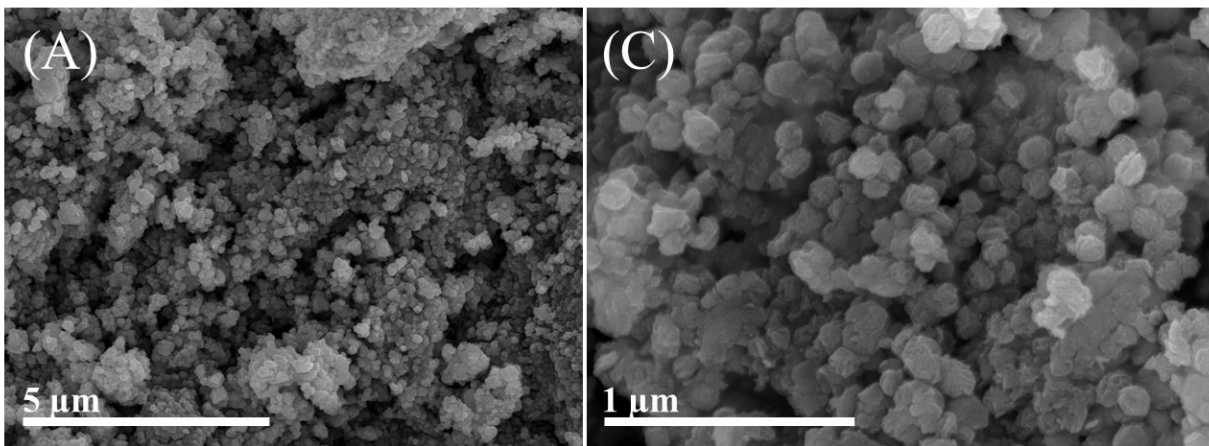


Fig. S5. SEM of the NiS@MoS₂/NC₁₀₀ composite at lower and higher magnification respectively.

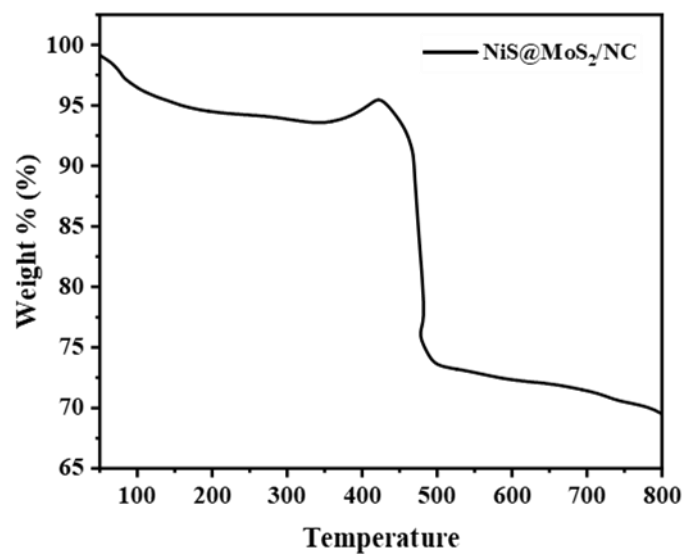


Fig. S6. TGA curves of the NiS@MoS₂/NC₅₀ composite.

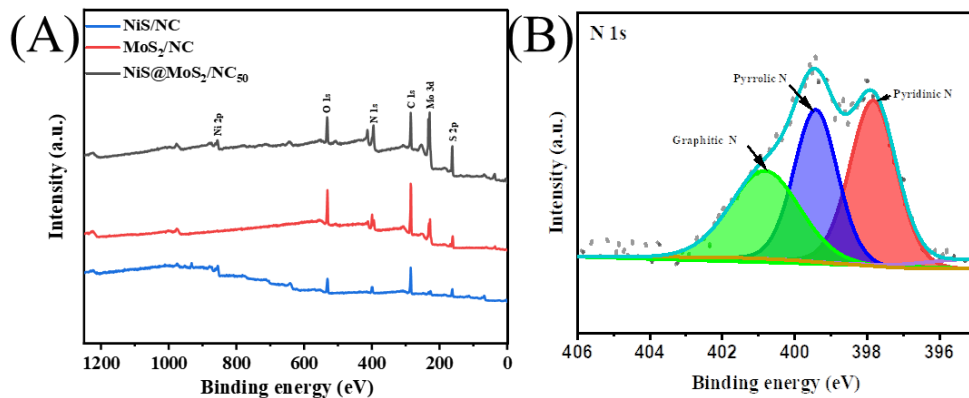


Fig. S7. (A). XPS survey spectra of NiS@MoS₂/NC₅₀, NiS/NC, and MoS₂/NC composites. (B). N spectra of NiS@MoS₂/NC₅₀.

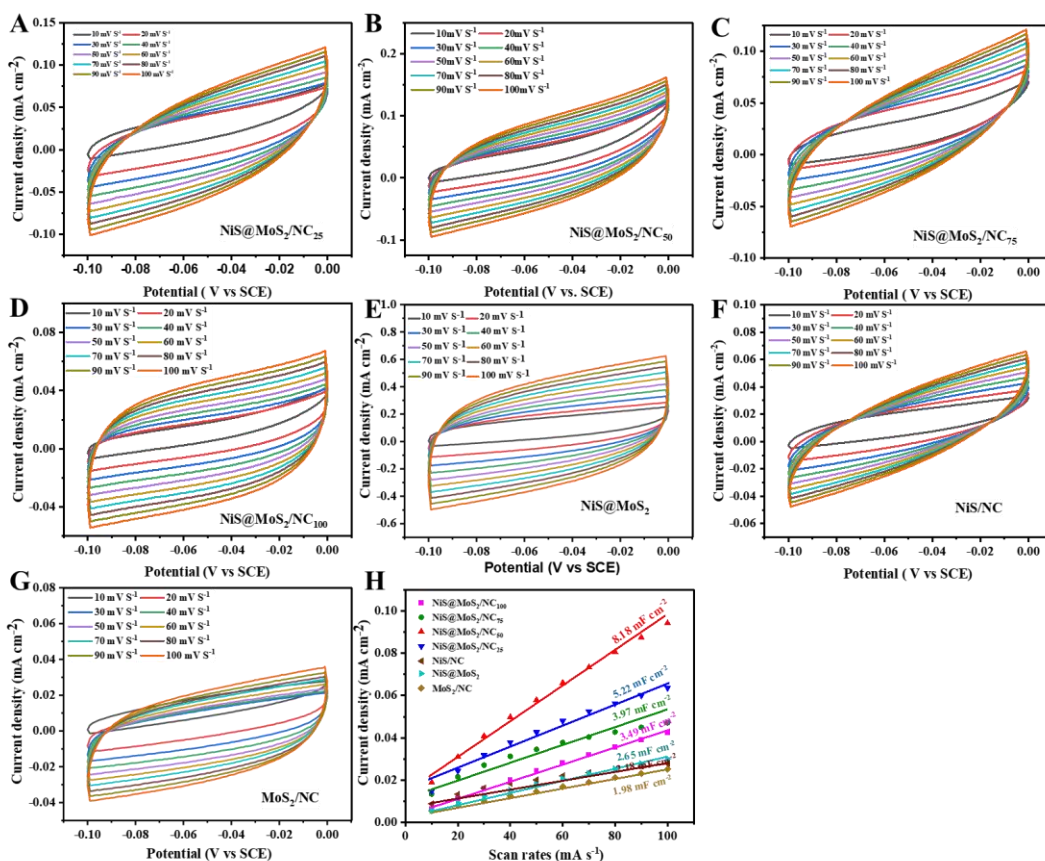


Fig. S8. (A-G) CV curves of the synthesized composites between -0.1 and 0 V vs. Hg/HgO at different scan rates in an acidic solution. (H) The C_{dl} values and determined by plotting the $\Delta J = (J_a - J_c)$ at -0.05 V vs. Hg/HgO against various scan rates, the C_{dl} is equal to the slop/2. The electrochemical surface area of catalysts can be determined from the C_{dl} .

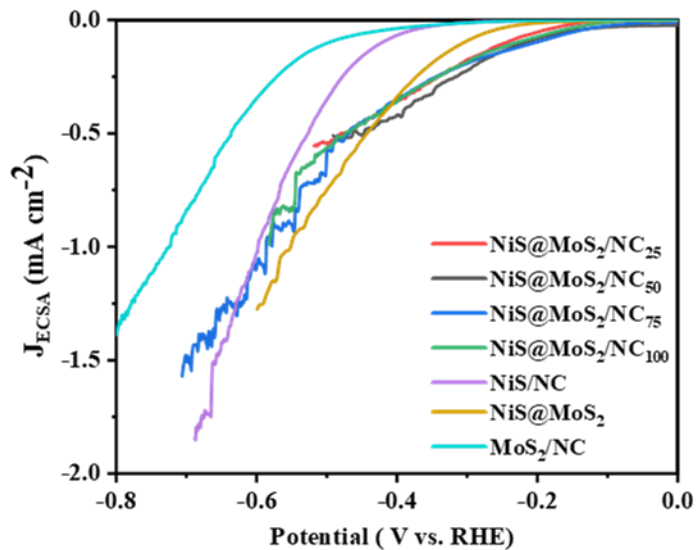


Fig. S9. ECSA normalized LSV curves of the as-prepared catalysts.

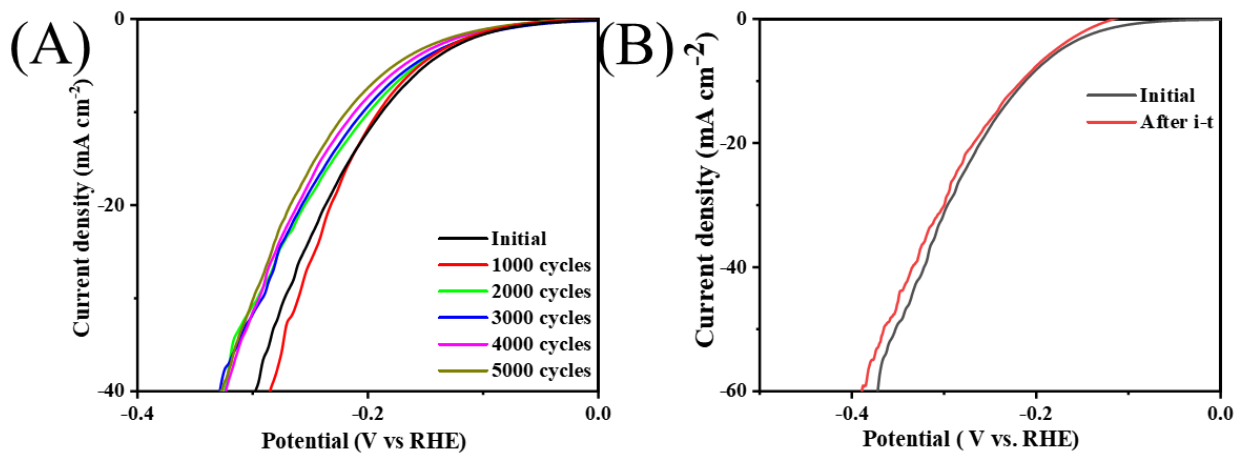


Fig. S10. LSV curves of the NiS@MoS₂/NC₅₀ catalyst after the cv cycles and before and after the i-t test.

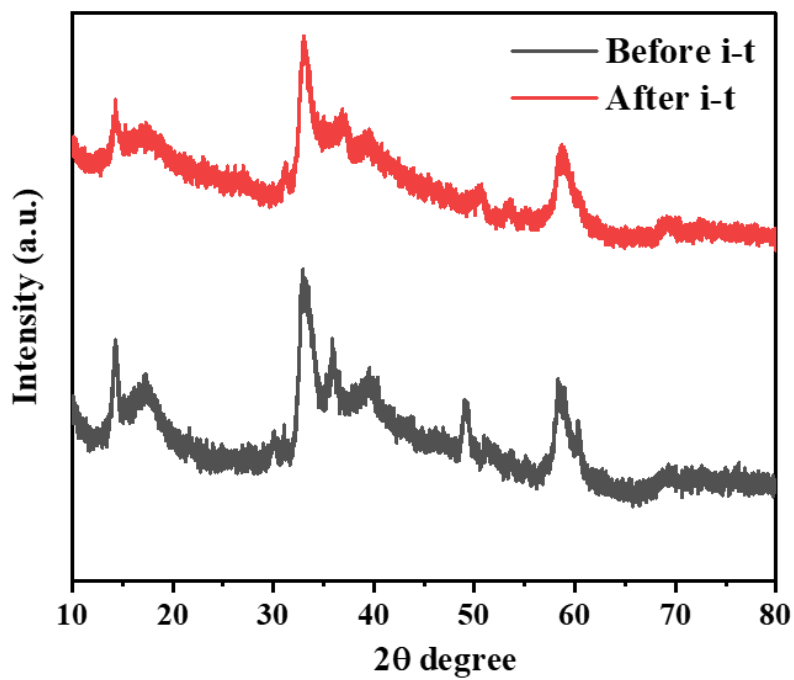


Fig. S11. XRD of the composite NiS@MoS₂/NC₅₀ before and after cv 5000 cycles.

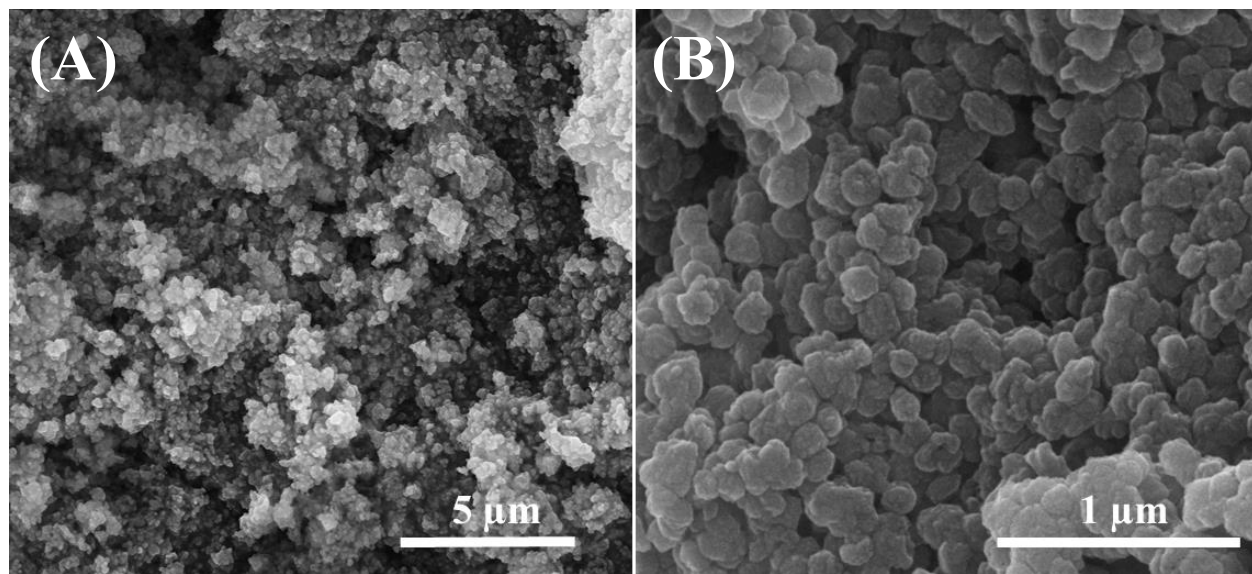


Fig. S12. SEM at lower and higher magnification of the NiS@MoS₂/NC₅₀ composite after cv 5000 cycles.

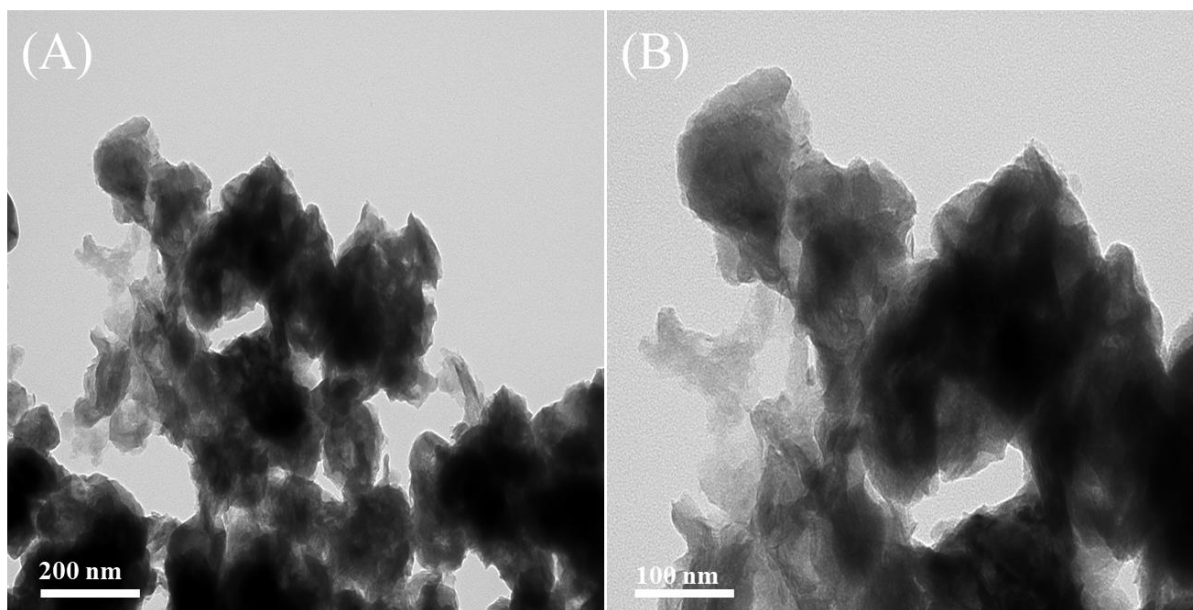


Fig. S13. TEM at lower and higher magnification of the NiS@MoS₂/NC₅₀ composite after cv 5000 cycles.

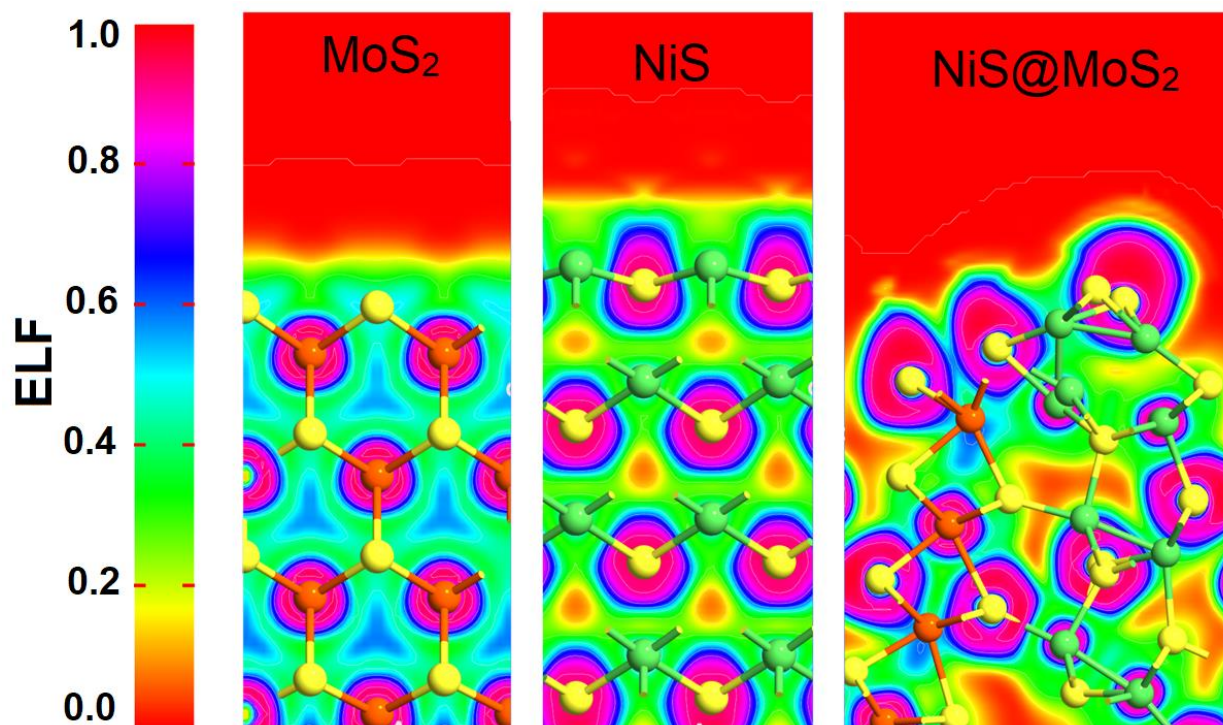


Fig. S14. Comparative ELF of MoS₂, NiS, and NiS@MoS₂ samples.

Table S1. The precursor composition for synthesis of catalysts.

Samples	Polyvinylpyrrolidone mg	NiSO ₄ · 6H ₂ O	CH ₄ N ₂ S	(NH ₄) ₆ Mo ₇ O ₂₄ ·4H ₂ O
		mg	mg	mg
NiS@MoS ₂ /NC ₂₅	200	50	1000	25
NiS@MoS ₂ /NC ₅₀	200	50	1000	50
NiS@MoS ₂ /NC ₇₅	200	50	1000	75
NiS@MoS ₂ /NC ₁₀₀	200	50	1000	100
NiS@MoS ₂	0	50	1000	50
MoS ₂ /NC	200	0	1000	50
NiS/NC	200	50	1000	0

Table S2. HER catalytic parameters of as-prepared and 20 % Pt/C catalysts.

Catalyst	(η)mV@(j)10mA cm ⁻²	Tafel slop (mV dec ⁻¹)	R _{ct} (Ω)	C _{dl} (mF cm ⁻²)
20%Pt/C	40	35.14	-	-
NiS@MoS ₂ /NC ₂₅	197	62.15	51.15	5.22
NiS@MoS ₂ /NC ₅₀	189	56.67	38.88	8.18

NiS@MoS ₂ /NC ₇₅	215	69.21	55.29	3.97
NiS@MoS ₂ /NC ₁₀₀	238	73.62	67.23	3.49
NiS@MoS ₂	333	91.63	204.3	2.18
NiS/NC	464	105.11	586.3	2.65
MoS ₂ /NC	555	128.54	737.2	1.98

Table S3. HER comparison performance of MoS₂-based catalysts.

Catalytic materials	Overpotential (mV) @10 mA cm ⁻²	Tafel slope (mV dec ⁻¹)	C _{dl} (mF cm ⁻²)	R _{ct} (Ω)	Ref.
NiS/MoS ₂ @CC	87	69.4	20.9	-	[1]
NiS@MoS ₂ Glassy carbon	152	66.5	75.32	194.9	[2]
MoS ₂ /NiS	244	97	13.86	-	[3]
MoS ₂ -NiS ₂ /NGF	172	70	25.1	-	[4]
1.0Ni-MoS ₂	173	69	-	-	[5]
Ni ₃ S ₂ /AT-Ni foam	200	107	-	-	[6]
NiCo ₂ S ₄ nanowires on Ni foam	210	58.9	-	18	[7]
Mo-Ni ₃ S ₂ /NF	216	104	45	-	[8]
N-rGO-MoS ₂ -Ni (OH) ₂	223	86.0	-	-	[9]

MoNiCNTs-4	238	84	-	-	[10]
NiMo ₃ S ₄	257	98	-	182	[11]
NiS@MoS ₂ /NC ₅₀	189	56.67	8.18	38.88	This work

REFERENCES

1. Gu, C., G. Zhou, J. Yang, H. Pang, M. Zhang, Q. Zhao, X. Gu, S. Tian, J. Zhang, L. Xu, and Y. Tang, NiS/MoS₂ Mott-Schottky heterojunction-induced local charge redistribution for high-efficiency urea-assisted energy-saving hydrogen production. *Chem. Eng. J.* 443 (2022) 136321. <https://doi.org/10.1016/j.cej.2022.136321>.
2. Chen, Z.W., X. Liu, P.J. Xin, H.T. Wang, Y. Wu, C.Y. Gao, Q.Q. He, Y. Jiang, Z.J. Hu, and S.S. Huang, Interface engineering of NiS@MoS₂ core-shell microspheres as an efficient catalyst for hydrogen evolution reaction in both acidic and alkaline medium. *J. Alloys Compd.* 853 (2021) 157352. <https://doi.org/10.1016/j.jallcom.2020.157352>.
3. Qin, Q., L.L. Chen, T. Wei, and X.E. Liu, MoS₂/NiS Yolk-Shell Microsphere-Based Electrodes for Overall Water Splitting and Asymmetric Supercapacitor. *Small.* 15 (2019) 1803639. <https://doi.org/10.1002/sml.201803639>.
4. Kuang, P., M. He, H. Zou, J. Yu, and K. Fan, 0D/3D MoS₂-NiS₂/N-doped graphene foam composite for efficient overall water splitting. *Appl. Catal. B.* 254 (2019) 15-25. <https://doi.org/10.1016/j.apcatb.2019.04.072>.
5. Luo, R., M. Luo, Z. Wang, P. Liu, S. Song, X. Wang, and M. Chen, The atomic origin of nickel-doping-induced catalytic enhancement in MoS₂ for electrochemical hydrogen production. *Nanoscale* 11 (2019) 7123-7128. <https://doi.org/10.1039/C8NR10023C>.

6. Ouyang, C., X. Wang, C. Wang, X. Zhang, J. Wu, Z. Ma, S. Dou, and S. Wang, Hierarchically Porous Ni₃S₂ Nanorod Array Foam as Highly Efficient Electrocatalyst for Hydrogen Evolution Reaction and Oxygen Evolution Reaction. *Electrochim. Acta.* 174 (2015) 297-301. <https://doi.org/10.1016/j.electacta.2015.05.186>.
7. Arumugam, S., P. Ganesan, and S. Shanmugam, Hierarchical NiCo₂S₄ nanowire arrays supported on Ni foam: An efficient and durable electrocatalyst for oxygen and hydrogen evolution reactions. *Adv. Funct. Mater.* 26 (2016) 4661-4672. <https://doi.org/10.1002/adfm.201600566>.
8. Gong, Y.Q., Y. Zhi, Y. Lin, T. Zhou, J.H. Li, F.X. Jiao, and W.F. Wang, Controlled synthesis of bifunctional particle-like Mo/Mn-NixSy/NF electrocatalyst for highly efficient overall water splitting. *Dalton Trans.* 48 (2019) 6718-6729. <https://doi.org/10.1039/C9DT00957D>.
9. Debata, S., S. Banerjee, and P.K. Sharma, Marigold shaped N-rGO-MoS₂-Ni(OH)₂ nanocomposite as a bifunctional electrocatalyst for the promotion of overall water splitting in alkaline medium. *Electrochim. Acta.* 303 (2019) 257-267. <https://doi.org/10.1016/j.electacta.2019.02.048>.
10. Zhang, X., P. Yang, and S.P. Jiang, Ni diffusion in vertical growth of MoS₂ nanosheets on carbon nanotubes towards highly efficient hydrogen evolution. *Carbon.* 175 (2021) 176-186. <https://doi.org/10.1016/j.carbon.2021.01.010>.
11. Jiang, J., M.R. Gao, W.C. Sheng, and Y.S. Yan, Hollow Chevrel-Phase NiMo₃S₄ for Hydrogen Evolution in Alkaline Electrolytes. *Angew. Chem. Int. Ed.* 55 (2016) 15240-15245. <https://doi.org/10.1002/anie.201607651>.